

## THE REDSHIFT OF THE BL LAC OBJECT TXS 0506+056.

SIMONA PAIANO,<sup>1,2</sup> RENATO FALOMO,<sup>1</sup> ALDO TREVES,<sup>3,4</sup> AND RICCARDO SCARPA<sup>5,6</sup>

<sup>1</sup>*INAF, Osservatorio Astronomico di Padova, Vicolo dell'Osservatorio 5 I-35122 Padova - ITALY*

<sup>2</sup>*INFN, Sezione di Padova, via Marzolo 8, I-35131 Padova - ITALY*

<sup>3</sup>*Università degli Studi dell'Insubria, Via Valleggio 11 I-22100 Como - ITALY*

<sup>4</sup>*INAF, Osservatorio Astronomico di Brera, Via E. Bianchi 46 I-23807 Merate (LC) - ITALY*

<sup>5</sup>*Instituto de Astrofísica de Canarias, C/O Via Lactea, s/n E38205 - La Laguna (Tenerife) - SPAIN*

<sup>6</sup>*Universidad de La Laguna, Dpto. Astrofísica, s/n E-38206 La Laguna (Tenerife) - SPAIN*

(Received February, 2018; Revised February 7, 2018; Accepted 2018)

Submitted to ApJL

### ABSTRACT

The bright BL Lac object TXS 0506+056 is a most likely counterpart of the IceCube neutrino event EHE 170922A. The lack of this redshift prevents a comprehensive understanding of the modeling of the source. We present high signal-to-noise optical spectroscopy, in the range 4100-9000 Å, obtained at the 10.4m Gran Telescopio Canarias. The spectrum is characterized by a power law continuum and is marked by faint interstellar features. In the regions unaffected by these features, we found three very weak ( $EW \sim 0.1$  Å) emission lines that we identify with [O II] 3727 Å, [O III] 5007 Å, and [NII] 6583 Å, yielding the redshift  $z = 0.3365 \pm 0.0010$ .

*Keywords:* galaxies: BL Lacertae objects: individual (TXS 0506+056) – distances and redshifts – gamma rays: galaxies –neutrinos

## 1. INTRODUCTION

The radio source TXS 0506+056 (3FGL J0509.4+0541) is a bright BL Lac object ( $V \sim 15$ ), that recently became of the utmost astrophysical interest since it is considered as the probable counterpart of the IceCube neutrino event EHE 170922A of 22 September 2017 (Kopper & Blaufuss 2017). This event is believed to be associated to enhanced  $\gamma$ -ray (100 MeV - 300 GeV) activity of the *Fermi*/LAT source 3FGL J0509.4+0541 (Tanaka et al. 2017; Lucarelli et al. 2017) and to a significant detection at  $> 100$  GeV by the MAGIC telescopes (Mirzoyan 2017). An enhanced flux was also revealed in the X-ray regime by the *Swift* satellite (Keivani et al. 2017) and from the ASAS-SN survey in the optical band (Franckowiak et al. 2017). During the event, the optical monitoring of the source indicates that the object was  $\sim 0.5$  mag brighter in the V band with respect to the earlier months.

Optical spectroscopy obtained in previous years by Halpern et al. (2003), Shaw et al. (2013) and Landoni et al. (2013), and after the neutrino event, failed to determine the redshift of this object (Steele 2017; Soelen et al. 2017; Coleiro & Chaty 2017; Morokuma et al. 2017).

Since the knowledge of the TXS 0506+056 distance is mandatory to model the spectral energy distribution and the neutrino production mechanism, we undertook a detailed spectroscopic study at the 10.4m Gran Telescopio Canarias (GTC).

Here we report the results obtained from high signal-to-noise optical observations aimed to pin down the redshift of the source.

## 2. OBSERVATIONS AND DATA ANALYSIS

TXS 0506+056 was observed with the GTC at the Roque de Los Muchachos with the spectrograph OSIRIS (Cepa et al. 2003) covering the spectral range 4100 - 9000 Å. We adopted different grisms (R1000 and R2500) yielding spectral

**Table 1.** LOG OF THE OBSERVATIONS

Grism	Date	Total exp. time (s)	N
R1000B	23-11-2017	3600	5
	05-12-2017	4200	6
R1000R	02-01-2018	4000	6
	14-01-2018	4000	6
R2500V	14-01-2018	4800	3
	14-01-2018	4800	3
R2500R	15-01-2018	4500	3
	20-01-2018	4800	6
R2500I	10-01-2018	4500	3
	13-01-2018	4500	2
	20-01-2018	4800	6

Col. 1: Grism name (slit width = 1.0" for R1000 and slit width = 1.2" for R2500); Col. 2: Date of the observation, Col. 3: Total exposure time, Col. 4: Number of individual exposures.

resolution  $R = \lambda/\Delta\lambda \sim 600$  and  $\sim 1300$ . For each setting, we obtained many independent exposures (see Tab. 1).

Data reduction was carried out using IRAF software and standard procedures for long slit spectroscopy, following the same scheme given in Paiano et al. (2017). The accuracy of the wavelength calibration is 0.1 Å. Relative flux calibration was derived from the observations of spectro-photometric standard stars.

For each dataset, we combined the independent exposures, weighting for signal-to-noise ratio (S/N), and anchored the absolute flux to the averaged magnitude of the source ( $g = 15.4$ ), as from the acquisition image. Finally the spectra were dereddened applying the extinction law by Cardelli et al. (1989), assuming  $E_{B-V} = 0.1$  as

**Table 2.** Optical spectral features

$\lambda$ (Å)	EW (Å)	ID
4190	$0.20 \pm 0.05$	DIB
4290	$0.15 \pm 0.05$	DIB
4427	$1.00 \pm 0.10$	DIB
4600	$0.30 \pm 0.07$	DIB
4770	$0.35 \pm 0.05$	DIB
4890	$0.30 \pm 0.06$	DIB
5780	$0.35 \pm 0.03$	DIB
4981.5	$0.12 \pm 0.03$	[OII] 3727Å
6693.6	$0.17 \pm 0.02$	[OIII] 5007Å
8800.5	$0.05 \pm 0.02$	[NII] 6583Å

Col. 1: Central wavelength of the feature; Col. 2: Observed equivalent width of the feature, Col. 3: Feature identification.

from the NASA/IPAC Infrared Science Archive [6](#)<sup>1</sup>.

### 3. RESULTS

In Fig. 1 we show the full  $R \sim 600$  optical spectrum. The S/N ranges from 650 to 1200 depending on the wavelength. The spectrum is characterized by a non-thermal emission with the power law shape ( $F_\lambda \propto \lambda^\alpha$ ) with spectral index of  $\alpha = -1.0 \pm 0.1$ .

Beside the prominent telluric absorptions and interstellar features, the whole optical spectrum does not exhibit emission or absorption lines with equivalent width  $> 0.5$  Å.

In order to evidentiate the spectral features, we divided it by a fit of the continuum, obtained excluding all regions affected by atmospheric and interstellar absorptions (see Fig. 2). From the normalized spectrum, we computed the nominal equivalent width (EW) in five intervals of the spectra, avoiding the prominent tel-

luric absorption features (see details about the used procedure in Appendix A in [Paiano et al. \(2017\)](#)). Five different intervals were considered because the S/N depends on the wavelength. This translates into a minimum ( $3\sigma$  level) detectable equivalent width:  $EW_{min} = 0.05 - 0.1$ .

The spectral region between 4100 Å and 4900 Å is affected by Diffuse Interstellar Bands (DIBs) (e.g. [Herbig 1995](#)) of  $EW = 0.3 - 1.0$  Å (see Table 2). In addition, the prominent ( $EW = 1.2$  Å) interstellar absorption line due to Na I 5892 Å is found<sup>2</sup>.

We search for weak intrinsic absorption and/or emission lines in the spectrum, avoiding all the interstellar spectral features and the regions clearly dominated by the telluric absorptions due to O<sub>2</sub> and H<sub>2</sub>O. We detect three faint narrow emission lines at  $4981.5 \pm 1.0$  Å,  $6693.6 \pm 1.1$  Å and at  $8800.5 \pm 1.1$  Å (see Fig. 2), identified as [OII] 3727 Å, [OIII] 5007 Å, and [NII] 6583 Å, respectively, at  $z = 0.336$ .

The presence of these three emission lines is also confirmed in the observations secured at  $R \sim 1300$  resolution (see Tab. 1). In Fig. 3, we reproduce the close-up of the spectral regions around the detected features. For these, we measured EW of  $0.12 \pm 0.03$  Å,  $0.17 \pm 0.02$  Å, and  $0.05 \pm 0.02$  Å, for [OII], [OIII], and [NII], respectively.

As a consistency check, we also estimate a redshift lower limit  $z > 0.3$ , based on the lack of absorption features due to the host galaxy, assuming to be a typical giant elliptical of  $M(R) = -22.9$  (see for details [Paiano et al. 2017](#)).

### 4. CONCLUSIONS

We obtained an unprecedented high S/N spectrum of the BL Lac object TXS 0506+056, that it is the likely counterpart of the Ice-Cube neutrino event. On the basis of three faint emission lines, we found the redshift is

<sup>1</sup> <http://irsa.ipac.caltech.edu/applications/DUST/>

<sup>2</sup> The source is at Galactic latitude  $l = -19.6^\circ$

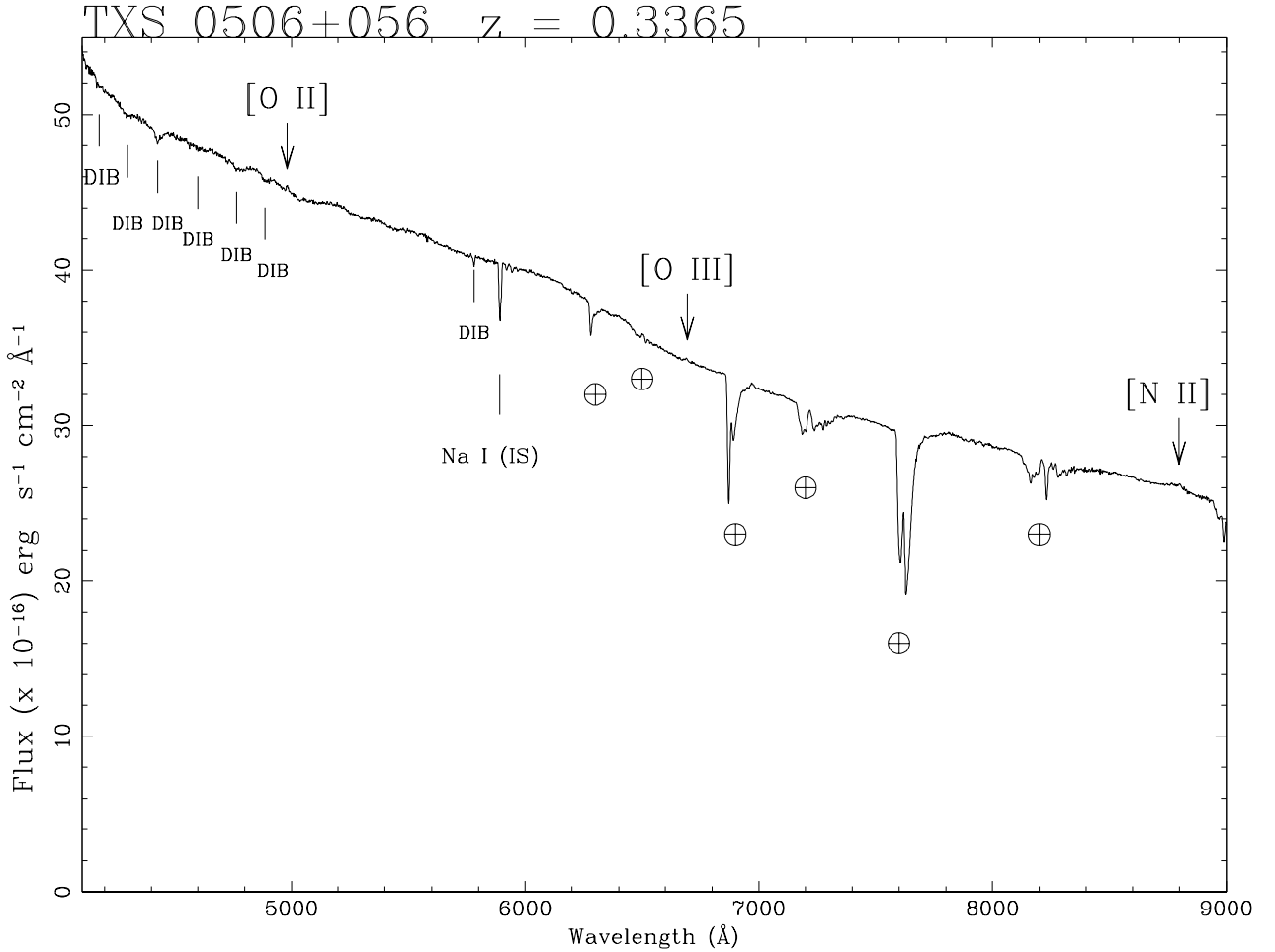


**Figure 1.** The optical spectrum of the BL Lac object TXS 0506+056 obtained at GTC+OSIRIS ( $R \sim 600$ ). The spectrum is corrected for reddening assuming  $E_{B-V} = 0.1$ . The shape of the spectrum is dominated by a non-thermal emission and the three arrows indicate the position of the detected emission lines at  $z = 0.3365$ . Absorption features due to interstellar medium are labelled as DIB and IS. The main telluric bands are marked by  $\oplus$ .

$z = 0.3365 \pm 0.0010$ . At this redshift the observed  $g$  luminosity is  $\nu L_\nu \sim 7 \times 10^{45}$  erg/s. Assuming that the source is hosted by a typical massive elliptical galaxy (e.g. Falomo et al. 2014), the magnitude is  $r(\text{host}) \sim 18.9$ . This translates into a total nucleus to host ratio  $> 10$  that is significantly larger than the average value found for BL Lac objects (see e.g. Scarpa et al. 2000) and it is indicative of an highly beamed source. The line luminosities are  $2.0 \times 10^{41}$  erg/s for the [OII] and [OIII]

and  $5.0 \times 10^{40}$  erg/s for the [NII]. The [OII] luminosity is typical of what is found in QSOs (see Kalfountzou et al. 2012). The line ratios  $\text{Log}([\text{OII}]/[\text{OIII}])$  and  $\text{Log}([\text{NII}]/[\text{OII}])$  are -0.15 and -0.38, respectively. These values are consistent with what typically found for narrow line region emission lines (Richardson et al. 2014). Neither the  $H_\beta$ , that would fall at  $\lambda \sim 6500$  Å where a weak telluric absorption is present, nor  $H_\alpha$  are detected in our spectra. The optical spectrum of TXS 0506+056 therefore resembles

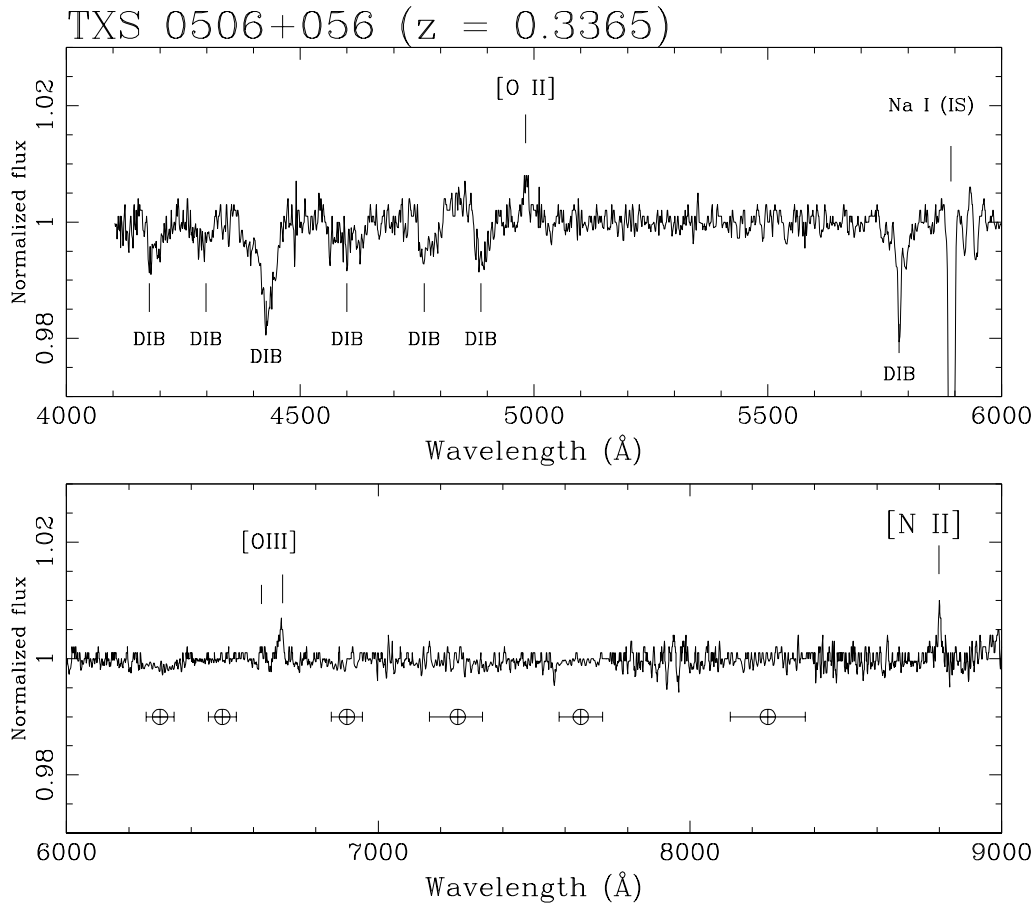


**Figure 2.** The normalized spectrum of the BL Lac object TXS 0506+056 (see also Fig.1). Three weak ( $EW \sim 0.1 \text{ \AA}$ ) emission lines are detected and identified as [OII] 3727 Å, [OIII] 5007Å, and [NII] 6583Å at the redshift  $z = 0.3365$ . Absorption features due to interstellar medium are labelled as DIB and IS. The spectral region affected by telluric absorptions, indicated by  $\oplus$ , were corrected.

that of a Seyfert 2 galaxy from the point of view of the emission lines. Based on the minimum EW in the regions of these two lines, we estimate that  $[OIII]/H_{\beta} \gtrsim 3$  while  $[NII]/H_{\alpha} \gtrsim 2$ . These ratios lead to interpret that these emission lines are originated in to the narrow line region of the AGN.

#### ACKNOWLEDGEMENT

We thank the referee for his/her prompt and constructive criticism and comments.

*Facilities:* GTC-OSIRIS, (Cepa et al. 2003)

*Software:* IRAF (Tody 1986, 1993)

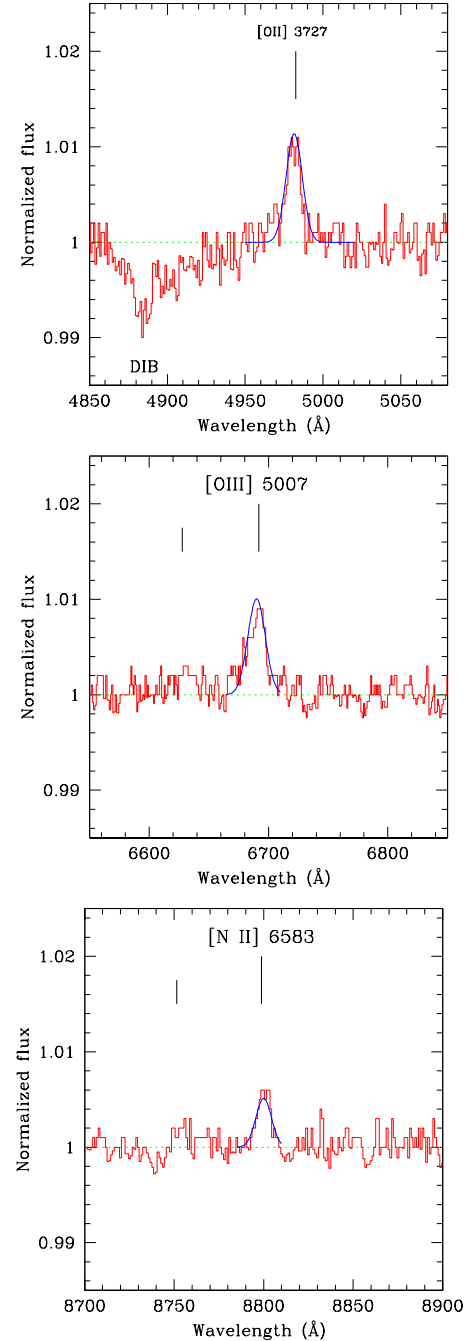


**Figure 3.** Close up of the normalized optical spectrum (obtained with  $R \sim 1300$ ) of TXS 0506+056 around the three faint detected emission lines. *Top:* The emission line at  $4981.5 \text{ \AA}$  identified as [OII]  $3727 \text{ \AA}$  ( $EW = 0.12 \text{ \AA}$ ). *Middle:* The emission line at  $6693.6 \text{ \AA}$  identified as [OIII]  $5007 \text{ \AA}$  ( $EW = 0.17 \text{ \AA}$ ), *Bottom:* The emission line at  $8800.5 \text{ \AA}$  identified as [NII]  $6583 \text{ \AA}$  ( $EW = 0.05 \text{ \AA}$ ). The short vertical bars indicate the fainter component of the doublet.

## REFERENCES

- Cardelli, J. A., Clayton, G. C., & Mathis, J. S. 1989, *ApJ*, 345, 245
- Cepa, J., Aguiar-Gonzalez, M., Bland-Hawthorn, J., et al. 2003, in *Proc. SPIE*, Vol. 4841, 1739–1749
- Coleiro, A., & Chaty, S. 2017, *The Astronomer’s Telegram*, 10840
- Falomo, R., Pian, E., & Treves, A. 2014, *A&A Rv*, 22, 73
- Franckowiak, A., Stanek, K. Z., Kochanek, C. S., et al. 2017, *The Astronomer’s Telegram*, 10794
- Halpern, J. P., Eracleous, M., & Mattox, J. R. 2003, *AJ*, 125, 572
- Herbig, G. H. 1995, *ARA&A*, 33, 19
- Kalfountzou, E., Jarvis, M. J., Bonfield, D. G., & Hardcastle, M. J. 2012, *MNRAS*, 427, 2401
- Keivani, P. A. E. A., Kennea, J. A., Fox, D. B., et al. 2017, *The Astronomer’s Telegram*, 10792
- Kopper, C., & Blaufuss, E. 2017, *GRB Coordinates Network, Circular Service*, No. 21916, #1 (2017), 21916
- Landoni, M., Falomo, R., Treves, A., et al. 2013, *AJ*, 145, 114
- Lucarelli, F., Piano, G., Pittori, C., et al. 2017, *The Astronomer’s Telegram*, 10801
- Mirzoyan, R. 2017, *The Astronomer’s Telegram*, 10817
- Morokuma, T., Tanaka, Y. T., Ohta, K., et al. 2017, *The Astronomer’s Telegram*, 10890
- Paiano, S., Landoni, M., Falomo, R., Treves, A., & Scarpa, R., 2017, *ApJ*, 837, 144
- Richardson, C. T., Allen, J. T., Baldwin, J. A., Hewett, P. C., & Ferland, G. J. 2014, *MNRAS*, 437, 2376
- Scarpa, R., Urry, C. M., Falomo, R., Pesce, J. E., & Treves, A. 2000, *ApJ*, 532, 740
- Shaw, M. S., Romani, R. W., Cotter, G., et al. 2013, *ApJ*, 764, 135
- Soelen, B. v., Buckley, D. A. H., & Boettcher, M. 2017, *The Astronomer’s Telegram*, 10830
- Steele, I. A. 2017, *The Astronomer’s Telegram*, 10799
- Tanaka, Y. T., Buson, S., & Kocevski, D. 2017, *The Astronomer’s Telegram*, 10791
- Tody, D. 1986, in *Proc. SPIE*, Vol. 627, *Instrumentation in astronomy VI*, ed. D. L. Crawford, 733
- Tody, D. 1993, in *Astronomical Society of the Pacific Conference Series*, Vol. 52, *Astronomical Data Analysis Software and Systems II*, ed. R. J. Hanisch, R. J. V. Brissenden, & J. Barnes, 173